Implicit Corotational Method: analysis of slender panels assemblages

Raffaele Casciaro [1], Stefano de Miranda[2], Antonio Madeo[1], Francesco Ubertini[2],Giuseppe Zagari[1]
[1] *MODELING, University of Calabria, Italy*
E-mail: rcasciaro@gmail, antoniomadeo@labmec.unical.it, giuseppe.zagari@gmail.com,

[2] *DISTART, University of Bologna, Italy*
E-mail: stefano.demiranda@unibo.it, francesco.ubertini@unibo.it

SUMMARY. In some recent works, it has been shown that the **Implicit Corotational Method** (or simply **ICM**) is a powerful and consolidated approach for recovering nonlinear models starting from the corresponding linear ones both in the cases of continuum and discrete problems (see [1, 2, 3]). The method is based on the polar decomposition theorem and the corotational description of motion, which is directly applied at the continuum level. By referring to the linear stress solution as Biot tensor in corotational frame and using a mixed variational formulation, we obtain an automated way of using the information gained by the linear model in the nonlinear context. Since linearized model are always available it is easy to obtain, by this way, the corresponding nonlinear models in a form convenient for numerical implementations. A similar picture holds when the approach is directly applied to the finite element discretization. In this case, starting from a linear finite element, the methods give the corresponding nonlinear, frame indifferent, finite element interpolation. As good and accurate is the linear finite element as good will be the corresponding nonlinear one.

On the other hand, in the last years high-performance plate finite elements, based on hybrid stress formulation and which exhibit a good behavior in the linear/elastic context, have been developed (see [4, 5, 6] and references therein) showing that they are in general simple, stable, locking–free. On the contrary, the developments of so good finite elements for the geometrically nonlinear case is in general more difficult.

The idea of the present work is then to reuse these finite elements in a nonlinear context using the **ICM**. For this purpose, the format of the element has been rearranged to be suitable for **ICM** implementation and a specialized corotational algebra for the plate model has been developed [7].

The implementations are carried out in both contexts of path–following and asymptotic approaches, extending the FE codes **KASP** and **RASP** already available and aimed at asymptotic and path–following analysis, respectively, of slender panels assemblages (see [8] and related references).

1 Implicit Corotational Method: FE implementation

The FE implementation of the nonlinear model recovered using the **ICM** can be performed through different kinds of interpolation strategies [3].

Once the continuum model is obtained, both Corotational (CR) or Total Lagrangian (TL) interpolations could be easily used in a standard fashion to produce a discrete model suitable for use in asymptotic and path–following solution strategies [9].

ICM allows the recovery of the mixed strain energy Φ, split in internal work $\mathcal{W}$ and complementary energy Φ_c of the nonlinear model, exploiting the kinematical relationship $\varrho[\bar{d}]$ in terms of

kinematical parameters $\bar{d}$ in the CR frame:

$$\Phi[\boldsymbol{t}, \bar{\boldsymbol{d}}] = \mathcal{W} - \Phi_c \ , \quad \mathcal{W} = \int_s \left\{ \boldsymbol{t}^T \boldsymbol{\varrho}[\bar{\boldsymbol{d}}] \right\} ds \ , \quad \Phi_c = \frac{1}{2} \int_s \left\{ \boldsymbol{t}^T \boldsymbol{H} \boldsymbol{t} \right\} ds \tag{1}$$

$\boldsymbol{t}$ being the stress parameters of the model, $\boldsymbol{H}$ the compliance operator and s being a suitable one or two dimensional abscissa. Using the geometrical relationships

$$\bar{\boldsymbol{d}} = \boldsymbol{g}[\boldsymbol{d}] \tag{2}$$

between kinematical parameters $\bar{\boldsymbol{d}}$ in CR frame and the corresponding ones in global fixed frame $\boldsymbol{d}$, the strain energy (1) can be expressed in terms of $\boldsymbol{d}$:

$$\Phi[\boldsymbol{t}, \boldsymbol{d}] = \int_s \left\{ \boldsymbol{t}^T \boldsymbol{\varrho}[\boldsymbol{d}] - \frac{1}{2} \boldsymbol{t}^T \boldsymbol{H} \boldsymbol{t} \right\} ds \tag{3}$$

Assuming an interpolation of generalized stress field defined by

$$\boldsymbol{t} = \boldsymbol{D}_t[s] \boldsymbol{t}_e$$

the discrete form Φ_{ce} of the complementary energy Φ_c becomes

$$\Phi_{ce}[\boldsymbol{t}_e] = \frac{1}{2} \boldsymbol{t}_e^T \boldsymbol{H}_e \boldsymbol{t}_e \ , \quad \boldsymbol{H}_e := \int_s \{ \boldsymbol{D}_t^T[s] \boldsymbol{H} \boldsymbol{D}_t[s] \} ds$$

$\boldsymbol{D}_t[s]$ being the operator collecting the interpolation functions and $\boldsymbol{t}_e$ the vector collecting the element stress parameters. The discrete form $\mathcal{W}_e$ of internal work $\mathcal{W}$ can be obtained in a different way depending on the motion description used, CR or TL.

1.1 Corotational interpolation

In this case the interpolation is performed on kinematical parameters $\bar{\boldsymbol{d}}$ in the CR frame:

$$\bar{\boldsymbol{d}} = \boldsymbol{D}_d[s] \bar{\boldsymbol{d}}_e \tag{4}$$

$\boldsymbol{D}_d[s]$ being the operator collecting the interpolation functions and $\bar{\boldsymbol{d}}_e$ the kinematical CR parameters of the element. Substituting the interpolation (4) into (2) and performing integration we obtain the following discrete internal work

$$\mathcal{W}_e[\boldsymbol{t}_e, \boldsymbol{\varrho}] = \boldsymbol{t}_e^T \boldsymbol{\varrho}_e[\bar{\boldsymbol{d}}_e] \ , \quad \boldsymbol{\varrho}_e[\bar{\boldsymbol{d}}_e] := \int_s \{ \boldsymbol{D}_t^T[s] \, \boldsymbol{\varrho} \, [\boldsymbol{D}_d[s] \bar{\boldsymbol{d}}_e] \} ds$$

The interpolation is completed exploiting the geometrical transformation law

$$\bar{\boldsymbol{d}}_e = \boldsymbol{g}_e[\boldsymbol{d}_e] \tag{5}$$

between discrete kinematical parameters $\bar{\boldsymbol{d}}_e$ in the CR frame and the corresponding ones in the global fixed frame $\boldsymbol{d}_e$. The aim of CR description is then to transfer the nonlinearity of the problem from the kinematical relationship to the geometrical transformation contained in eq. (5). As the frame indifference requirements is guaranteed 'a priori' in terms of the rotation defining the CR frame, by the geometric laws eq.(5), the interpolation matrix $\boldsymbol{D}_d[s]$ could be the same used for the corresponding linear FE interpolation of the model. Furthermore as in this context the finite element kinematical descriptor $\bar{\boldsymbol{d}}_e$ is also small, the discrete strain measure $\boldsymbol{\varrho}[\bar{\boldsymbol{d}}_e]$ can be expanded using Taylor expansion (see [7] for further details), without any loss in accuracy. Usually linear or quadratic expansions are used in this respect while the improvement in of accuracy is demanded for a refinement of the finite element mesh that is to a local better evaluation of $\boldsymbol{Q}$. Note that:

- when $\boldsymbol{D}_d[s]$ is assumed to be the same as the linear finite element model and $\boldsymbol{\varrho}_e[\bar{\boldsymbol{d}}_e]$ is linearized in terms of $\bar{\boldsymbol{d}}_e$ we obtain the "standard" form of the CR formulation [13] that allows us to obtain, in an easy way, a nonlinear finite element starting from the corresponding linear one;

- the evaluation of the CR frame could be not constant on the element and, for example, evaluated in a series of Gauss points for a better elimination of the mean rigid body motion. This requires the integral in eq. (1) and the geometric law (2) to be split.

1.2 Total Lagrangian interpolation

In this strategy we interpolate the global kinematical parameters $\boldsymbol{d}$

$$\boldsymbol{d} = \boldsymbol{D}_d[s]\boldsymbol{d}_e$$

$\boldsymbol{D}_d[s]$ and $\boldsymbol{d}_e$ being the operator containing the interpolation functions and $\boldsymbol{d}_e$ the vector collecting the finite element kinematical parameters. The internal work (3) then becomes:

$$\mathcal{W}_e[\boldsymbol{t}_e, \boldsymbol{\varrho}_e] = \boldsymbol{t}_e^T \boldsymbol{\varrho}_e[\boldsymbol{d}_e] \ , \quad \boldsymbol{\varrho}_e[\boldsymbol{d}_e] := \int_s \{\boldsymbol{D}_t^T[s]\, \boldsymbol{\varrho}\,[\boldsymbol{D}_d[s]\boldsymbol{d}_e]\}ds$$

In particular, it is well known (see [14] and references therein) that to obtain a frame indifferent model the finite element interpolation also needs to be frame indifferent, so the choice of the interpolation functions contained in $\boldsymbol{D}_d[s]$ is in general important.

2 The *standard* Corotational formulation

As stated in the above discussion, the *standard* CR approach as proposed by Rankin [13] is fully placed into the ICM.

The CR description of motion has its origins in the polar decomposition theorem (see [11]). According to this theorem, the total deformation of a continuous body can be decomposed into a rigid body motion and a local deformation. In FE implementation, this decomposition can be performed using a local CR frame that rotates and translates with each element. The advantage is that the nonlinearity of the problem is transferred to the coordinate change between the fixed and corotational systems, and the local displacements can be assumed small enough, in the CR frame, to allow strains to be obtained through linear or a simplified nonlinear strain–displacement relationships, without introducing significant errors. In fact, the strain energy thus obtained proves to be objective with respect to rigid body motions of the element, exactly, and the residual error coming from the simplified local description of the element can always be made small enough by a mesh refinement. The main advantage of this approach is that we can reuse standard finite element libraries [13] thereby avoiding the need for objective interpolations [14] as occurs in other descriptions of the body motion. The nonlinearity of the problem is essentially transferred to the relationship between global and local components of the nodal displacements, which is governed by a simple kinematics and does not present particular difficulties, apart from that due to the presence of nodal rotational variables. The CR approach has been widely used as a basic tool for describing the configuration changes within incremental–iterative path–following analysis. In this context, it requires the evaluation of the first two variations of the strain energy. Only the first variation, used for checking the equilibrium, actually needs to be evaluated exactly. Even a rough estimate for the second one is generally sufficient, because it is only employed for defining a suitable iteration matrix to be used within a Newton–like solution process [13]. The overall picture changes when using the asymptotic

approach. All quantities which define the configuration state are obtained through a direct extrapolation, thereby reducing or completely eliminating, the need for an updating process. Nonetheless, an accurate evaluation for the first four variations of strain energy is needed.

2.1 Corotational algebra: Strain energy in the CR frame

Consider the motion described by the point displacement $\boldsymbol{u}[\boldsymbol{X}]$ and rotation $\boldsymbol{\varphi}[\boldsymbol{X}]$ vector fields, $\boldsymbol{X}$ being the position of the point in the reference configuration with respect to the fixed frame. Using simple geometric considerations and omitting the dependence on $\boldsymbol{X}$, for an easy notation, the deformational local part of $\boldsymbol{u}[\boldsymbol{X}]$ can be described by the expressions

$$\bar{\boldsymbol{u}} = \boldsymbol{Q}^T[\boldsymbol{\alpha}](\boldsymbol{X} + \boldsymbol{u} - \boldsymbol{c}) - \boldsymbol{X} \tag{6}$$

where $\boldsymbol{Q}[\boldsymbol{\alpha}]$ is the matrix rotation defining CR frame, $\boldsymbol{\alpha}$ being the axial rotation vector associate to $\boldsymbol{Q}$ through Rodrigues parametrization [12], $\boldsymbol{c}$ is the translation of the CR frame and $\bar{\boldsymbol{u}}$ collects the components of the deformational displacement. Similarly, the rotation vector of the local part of point rotation $\boldsymbol{R}[\boldsymbol{\varphi}]$, $\boldsymbol{\varphi}$ being the axial rotation associate to $\boldsymbol{R}$ through Rodrigues formula, expressed by

$$\bar{\boldsymbol{\varphi}} = \log(\bar{\boldsymbol{R}}) \quad \text{with} \quad \bar{\boldsymbol{R}} = \boldsymbol{Q}^T \boldsymbol{R} \tag{7}$$

defining with $\log[\cdot]$ the extraction of the axial vector from a matrix rotation.

The point strain will be a function of the deformational displacement and rotation $\bar{\boldsymbol{d}} = \{\bar{\boldsymbol{u}}, \bar{\boldsymbol{\varphi}}\}$:

$$\boldsymbol{\varrho} = \boldsymbol{\varrho}[\bar{\boldsymbol{d}}]$$

Assuming that $\bar{\boldsymbol{d}}$ and $\bar{\boldsymbol{\varphi}}$ are small, the constitutive laws can be taken as linear. It is then possible to express the finite element strain energy, in mixed form, as (see (1))

$$\Phi[u] = \int_s \left\{ \boldsymbol{t}^T \boldsymbol{\varrho}[\bar{\boldsymbol{d}}] - \frac{1}{2} \boldsymbol{t}^T \boldsymbol{H} \boldsymbol{t} \right\} ds \tag{8}$$

Exploiting the element interpolation laws (see (4)), (8) can be rewritten, in discrete form, as:

$$\Phi_e[u] := \boldsymbol{t}_e^T \boldsymbol{\varrho}_e[\bar{\boldsymbol{d}}_e] - \frac{1}{2} \boldsymbol{t}_e^T \boldsymbol{H}_e \boldsymbol{t}_e$$

$\boldsymbol{t}_e$ being the vector of the element stress parameters and $\boldsymbol{\varrho}$ the associated vector of the strains, as a function of the displacement element vector $\bar{\boldsymbol{d}}_e$ collecting deformational displacements $\bar{\boldsymbol{d}}_k$ and rotations $\bar{\boldsymbol{\varphi}}_k$ of all k–th finite element nodes (or a relevant linear combination of them). Finally $\boldsymbol{H}_e$ is the Clapeyron compliance matrix provided by the complementary energy equivalence

$$\frac{1}{2} \boldsymbol{t}_e^T \boldsymbol{H}_e \boldsymbol{t}_e = \frac{1}{2} \int_s \boldsymbol{t}^T \boldsymbol{H} \boldsymbol{t} \, ds \quad , \quad \forall \boldsymbol{t}_e, \, \boldsymbol{t}[\boldsymbol{t}_e]$$

Exploiting the smallness of deformational displacements, we assume that $\boldsymbol{\varrho}$ can have, at most, the following linear expression in terms of $\bar{\boldsymbol{d}}_e$:

$$\boldsymbol{\varrho}[\bar{\boldsymbol{d}}_e] = \boldsymbol{D}\bar{\boldsymbol{d}}_e$$

The discrete expression of the strain energy (8) becomes

$$\Phi[u] = \boldsymbol{t}_e^T \boldsymbol{D}\bar{\boldsymbol{d}}_e - \frac{1}{2} \boldsymbol{t}_e^T \boldsymbol{H}_e \boldsymbol{t}_e \tag{9}$$

Letting $\boldsymbol{\alpha}_e$ be the CR rotation vector associated to the average rigid rotation of the element and

$$\boldsymbol{Q}_e \equiv \boldsymbol{Q}[\boldsymbol{\alpha}_e]$$

the CR formulation is based on two fundamental steps:

a) the definition of kinematical relationships (6) and (7) that express a purely *geometric nonlinear relation*

$$\bar{\boldsymbol{d}}_e = \boldsymbol{g}_e[\boldsymbol{\alpha}_e, \boldsymbol{d}_e] \tag{10}$$

between the element displacement vector in the CR ($\bar{\boldsymbol{d}}_e$) and fixed frames ($\boldsymbol{d}_e$).

b) a *local modeling* of the mechanical behavior of the structures, which is an implicitly defined expression of the strain energy of the element in terms of local CR finite element parameters, which is written in the simplified form (9), because of the assumption of small local displacements.

Note that the geometrical nonlinearities are essentially contained in eq. (10), while the local modeling only implies standard finite element procedures and, if using expression (9), corresponds to a linear FE modeling. The corotational approach then leads to an efficient way of reusing standard FE technology in a nonlinear context.

2.2   Strain energy in the fixed frame

The CR rotation vector $\boldsymbol{\alpha}_e$ will be a function of the current displacement vector $\boldsymbol{d}_e$:

$$\boldsymbol{\alpha}_e = \boldsymbol{\alpha}_e[\boldsymbol{d}_e] \tag{11}$$

The explicit expression of this function will depend on the particular element which is used and is based on the best compromise between algebraic simplicity and accuracy, the latter being essentially related to the smallness of the deformational part of the motion. By substituting eq. (11) into (10), we can express $\bar{\boldsymbol{d}}_e$ as a function of $\boldsymbol{d}_e$ alone:

$$\bar{\boldsymbol{d}}_e = \boldsymbol{g}_e[\boldsymbol{d}_e]$$

The combination of eqs. (9) and (10) allows the element energy to be expressed in terms of the element vector

$$\boldsymbol{u}_e = \{\boldsymbol{t}_e, \boldsymbol{d}_e\}$$

which collects all parameters defining the element configuration in a single vector and can be related to the global vector $\boldsymbol{u}$, expressing the overall configuration of the assemblage, through the known relation

$$\boldsymbol{u}_e = \boldsymbol{A}_e \boldsymbol{u}$$

where matrix $\boldsymbol{A}_e$ implicitly contains the link constraints between elements. This allows the energy to be expressed as an algebraic nonlinear function of $\boldsymbol{u}$:

$$\Phi[u] = \sum_e \Phi_e[u] \tag{12}$$

Once obtained the algebraic expression of the strain energy (12), the scalar and vectorial quantities needing for the asymptotic and path–following analyses can be performed following the algebraic scheme proposed into [7].

3   Energy variations: second variations using linear local modeling

We will denote with u_i ($i = 1 \ldots 4$) a generic variation of the configuration field u, with $\boldsymbol{u}_i$ the corresponding global configuration vector in the FE discrimination and with $\boldsymbol{u}_{ie} = \boldsymbol{A}_e \boldsymbol{u}_i$ the finite element configuration vector collecting both displacement and stress element vectors: $\boldsymbol{u}_{ie} = \{\boldsymbol{t}_{ie}, \boldsymbol{d}_{ie}\}^T$. With the same notation $\boldsymbol{u}_0$ and $\boldsymbol{u}_{0e}$ are the global and element reference configuration vectors.

Second energy can be expressed as

$$\Phi_e^{''} u_1 u_2 = \boldsymbol{t}_{1e}^T \boldsymbol{\varrho}_{1e}[\boldsymbol{d}_{2e}] + \boldsymbol{t}_{2e}^T \boldsymbol{\varrho}_{1e}[\boldsymbol{d}_{2e}] - \boldsymbol{t}_{1e}^T \boldsymbol{H}_e \boldsymbol{t}_{2e} + \boldsymbol{t}_{0e}^T \boldsymbol{\varrho}_{2e}[\boldsymbol{d}_{1e}, \boldsymbol{d}_{2e}] \tag{13a}$$

where $\boldsymbol{\varrho}_{1e}$ and $\boldsymbol{\varrho}_{2e}$ are defined by

$$\boldsymbol{\varrho}_{1e}[\boldsymbol{d}_{je}] = \boldsymbol{D}\boldsymbol{g}_{1e}[\boldsymbol{d}_{je}] \qquad \boldsymbol{\varrho}_{2e}[\boldsymbol{d}_{1e}, \boldsymbol{d}_{2e}] = \boldsymbol{D}\boldsymbol{g}_{2e}[\boldsymbol{d}_{1e}, \boldsymbol{d}_{2e}] \qquad j = 1, 2 \tag{13b}$$

Introducing the matrices $\boldsymbol{L}_1$ and $\boldsymbol{G}[\boldsymbol{t}_e]$ through the following equivalences

$$\boldsymbol{L}_1 \boldsymbol{d}_{je} = \boldsymbol{g}_{1e}[\boldsymbol{d}_{je}] \;\;, \;\; \boldsymbol{d}_{1e}^T \boldsymbol{G}[\boldsymbol{t}_{0e}] \boldsymbol{d}_{2e} = \boldsymbol{t}_{0e}^T \boldsymbol{\varrho}_{2e}[\boldsymbol{d}_{1e}, \boldsymbol{d}_{2e}] \tag{14}$$

eq. (13) can be rearranged in a more convenient compact form:

$$\Phi_e^{''} u_1 u_2 = \boldsymbol{u}_{1e}^T \boldsymbol{H}_e \boldsymbol{u}_{2e} \;\;, \;\; \boldsymbol{H}_e = \begin{bmatrix} -\boldsymbol{K}_c^{-1} & \boldsymbol{D}\boldsymbol{L}_1 \\ \boldsymbol{L}_1^T \boldsymbol{D}^T & \boldsymbol{G}[\boldsymbol{t}_{0e}] \end{bmatrix} \tag{15}$$

The mixed tangent matrix of the element $\boldsymbol{H}_e$ can be directly used, through a standard assemblage process, to obtain the overall Hessian matrix $\boldsymbol{H}$:

$$\Phi^{''} u_1 u_2 = \boldsymbol{u}_1^T \boldsymbol{H} \boldsymbol{u}_2 \;\;, \;\; \boldsymbol{H} := \sum_e \boldsymbol{A}_e^T \boldsymbol{H}_e \boldsymbol{A}_e \tag{16}$$

3.1   Third variations using linear modeling

The element contribution to the scalar expressions is easily evaluated using the general formula

$$\Phi_e^{'''} u_1 u_2 u_3 = \boldsymbol{t}_{1e}^T \boldsymbol{\varrho}_{2e}[\boldsymbol{d}_{2e}, \boldsymbol{d}_{3e}] + \boldsymbol{t}_{2e}^T \boldsymbol{\varrho}_{2e}[\boldsymbol{d}_{3e}, \boldsymbol{d}_{1e}] + \boldsymbol{t}_{3e}^T \boldsymbol{\varrho}_{2e}[\boldsymbol{d}_{1e}, \boldsymbol{d}_{2e}] + \boldsymbol{t}_{0e}^T \boldsymbol{\varrho}_{3e}[\boldsymbol{d}_{1e}, \boldsymbol{d}_{2e}, \boldsymbol{d}_{3e}] \tag{17}$$

where $\boldsymbol{\varrho}_{2e}[\cdot, \cdot]$ is defined by (13b) and $\boldsymbol{\varrho}_{3e}[\cdots]$ is obtained by

$$\boldsymbol{\varrho}_{3e}[\boldsymbol{d}_{1e}, \boldsymbol{d}_{2e}, \boldsymbol{d}_{3e}] = \boldsymbol{D}\boldsymbol{g}_{3e}[\boldsymbol{d}_{1e}, \boldsymbol{d}_{2e}, \boldsymbol{d}_{3e}]$$

When the vectorial expression is needed, making $u_3 = \delta u$, eq. (17) can be rearranged in the form

$$\Phi_e^{'''} u_1 u_2 \delta u := \delta \boldsymbol{u}_e^T \boldsymbol{s}_e = \begin{bmatrix} \delta \boldsymbol{t}_e \\ \delta \boldsymbol{d}_e \end{bmatrix}^T \begin{bmatrix} \boldsymbol{s}_{et} \\ \boldsymbol{s}_{ed} \end{bmatrix}$$

where $\boldsymbol{s}_{et} := \boldsymbol{\varrho}_{2e}[\boldsymbol{d}_{1e}, \boldsymbol{d}_{2e}]$ and $\boldsymbol{s}_{ed}$ is defined by the equivalence

$$\delta \boldsymbol{d}_e^T \boldsymbol{s}_{ed} = \delta \boldsymbol{d}_e^T (\boldsymbol{G}[\boldsymbol{t}_{1e}] \boldsymbol{d}_{2e} + \boldsymbol{G}[\boldsymbol{t}_{2e}] \boldsymbol{d}_{1e}) + \boldsymbol{t}_{0e}^T \boldsymbol{\varrho}_{3e}[\boldsymbol{d}_{1e}, \boldsymbol{d}_{2e}, \delta \boldsymbol{d}_e]$$

The overall vector $\boldsymbol{s}$ is then obtained by a standard assemblage

$$\boldsymbol{s}[\boldsymbol{u}_1, \boldsymbol{u}_2] = \sum_e \boldsymbol{A}_e^T \boldsymbol{s}_e[\boldsymbol{u}_{1e}, \boldsymbol{u}_{2e}]$$

3.2 Fourth variations using linear local modeling

The following general formula for the element contributions can be used.

$$\Phi_e^{''''} u_1 u_2 u_3 u_4 = \boldsymbol{t}_{1e}^T \boldsymbol{\varrho}_{3e}[\boldsymbol{d}_{2e}, \boldsymbol{d}_{3e}, \boldsymbol{d}_{4e}] + \boldsymbol{t}_{2e}^T \boldsymbol{\varrho}_{3e}[\boldsymbol{d}_{3e}, \boldsymbol{d}_{4e}, \boldsymbol{d}_{1e}]$$
$$+ \boldsymbol{t}_{3e}^T \boldsymbol{\varrho}_{3e}[\boldsymbol{d}_{4e}, \boldsymbol{d}_{1e}, \boldsymbol{d}_{2e}] + \boldsymbol{t}_{4e}^T \boldsymbol{\varrho}_{3e}[\boldsymbol{d}_{1e}, \boldsymbol{d}_{2e}, \boldsymbol{d}_{3e}]$$
$$+ \boldsymbol{t}_{0e}^T \boldsymbol{\varrho}_{4e}[\boldsymbol{d}_{1e}, \boldsymbol{d}_{2e}, \boldsymbol{d}_{3e}, \boldsymbol{d}_{4e}]$$

where function $\boldsymbol{\varrho}_{4e}[\cdot]$ is obtained by

$$\boldsymbol{\varrho}_{4e}[\boldsymbol{d}_{1e}, \boldsymbol{d}_{2e}, \boldsymbol{d}_{3e}, \boldsymbol{d}_{4e}] = \boldsymbol{D}\boldsymbol{g}_{4e}[\boldsymbol{d}_{1e}, \boldsymbol{d}_{2e}, \boldsymbol{d}_{3e}, \boldsymbol{d}_{4e}].$$

4 Finite element in CR frame for the analysis of plate assemblages

The nonlinear analysis of plate frames have been carried out reusing the mixed finite elements which exhibit a good behavior in the linear/elastic context. The following compromise have been made. For the membrane behaviour a 4-node finite elements is adopted (see [6, 10] and references therein). The element assumes bilinear shape function for the in–plane displacements on the element domain and quadratic shape function along the edges, then additional in plane rotation are used as kinematical parameters. The stress interpolation is controlled by nine stress parameters. The bending behaviour is modeled trough a 4-node element (see [4, 5] and references therein), based on the hybrid stress formulation. The element, in linear context, is designed to be simple, stable, free of locking and to pass all the patch tests. The standard displacement interpolation is enhanced by linking the transverse displacement to the nodal rotations and an appropriate stress approximation is rationally derived. In particular, the assumed stress approximation is equilibrated within each element, co-ordinate invariant and ruled by the minimum number of parameters. This element is isostatic and is based on nine stress parameters.

5 Numerical results

Some numerical benchmarks are here proposed to check the accuracy of the proposed approach.

5.1 Euler beam and Roorda frame

The first test are the Euler beam and Roorda frame. The geometry of the tests can be found into the paper [1]. The buckling values λ_b are compared for different mesh (see tables (1,2)).

mesh	regular	irregular
1×10	9.9483	10.0449
2×20	9.8881	9.9123
4×40	9.8730	9.8789
8×80	9.8690	9.8705
Ref. sol.	9.8694	

Table 1: λ_b, Euler beam

5.2 **C**-shaped beam under axial force

The geometry of the test can be found into the paper [15]. The flexural–torsional behaviour is outlined. The buckling values λ_b are reported and compared also with commercial codes (see table(3) and figures (1,2)).

7

elements	regular	irregular
1×10	14.009	14.164
2×20	13.912	13.956
4×40	13.894	13.903
Ref. sol.	13.886	

Table 2: λ_b, Roorda frame

mesh	1st mode	2nd mode
coarse	0.871	11.01
fine	0.874	11.38
Abaqus	0.876	11.87
Kasp	0.874	11.96

Table 3: λ_b, **C**–shaped beam

6   Concluding remarks

A FE implementation of **ICM** in the context of plate assemblages have been presented. A general tool for evaluating energy variations aimed at path–following and asymptotic analyses has been developed. The implementation use extensively corotational algebra and then the decoupling of pure deformational and geometrically part of the motion. High–performance mixed elements have been used for the analysis [4, 6]. This choice is a good compromise of element simplicity and accuracy. However the developed tool is quite general and allows to change in–plane and out–plane finite elements with few modifications. Note that the implementations are carried out extending the FE codes **KASP** and **RASP** already available [8] and aimed to asymptotic and path–following analysis respectively of slender panels assemblages. Finally, the results show the reliability and the accuracy of the proposed approach.
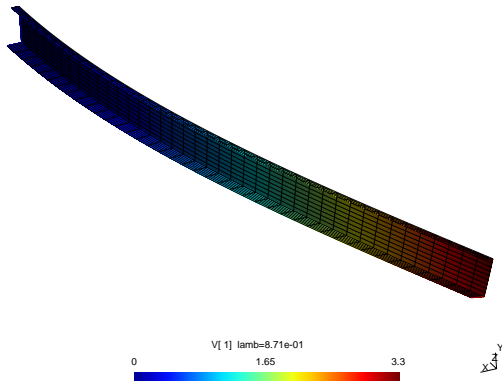
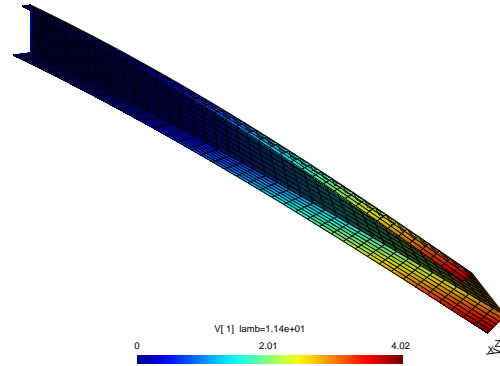Figure 1: **C**-shaped beam under axial force. 1th buckling mode

Figure 2: **C**-shaped beam under axial force. 2th buckling mode

References

[1] G. Garcea, A. Madeo, 'Rational strain measures - The Implicit Corotational Method', ECCM - 2006 Lisbon.

[2] R. Casciaro, G. Garcea, A. Madeo, 'Elastic postbuckling analysis: how to recover accurate nonlinear structural models from the linear ones', WCCM - 2008 Venice.

[3] A. Madeo, 'The Implicit Corotational Method: General theory and FEM implementation', Ph.d Thesis, University of Calabria, 2009. http://www.labmec.unical.it/pubblicazioni/dottorato.php.

[4] S. de Miranda, F. Ubertini, 'A simple hybrid stress element for shear deformable plates', International Journal for Numerical Methods in Engineering, **65**, 808–833, (2006).

[5] F. Daghia, S. de Miranda, F. Ubertini, E. Viola, 'A hybrid stress approach for laminated composite plates whitin the First-order Shear Deformation Theory', International Journal of Solids and Structures, **45**, 1766–1787, (2008).

[6] G. Rengarajan, M.A. Aminpour, N.F. Knight,'Improved assumed stress hybrid shell element with drilling degrees of freedom for linear stress, buckling, and free vibration anlyses'. NASA-CR-192816.

[7] G. Garcea, A. Madeo, G. Zagari, R. Casciaro, 'Asymptotic post–buckling FEM analysis using a corotational formulation', Int. Journal of Solids & Structures **46** (2), 523–532, (2009).

[8] G. Garcea, 'Mixed formulation in Koiter analysis of thin walled beam', Computer Methods in Applied Mechanics and Engineering, **190**, 3369-3399, (2001).

[9] G.Garcea, A. Madeo, G. Zagari, 'The Implicit Corotational Method: FEM implementation'. ECSM - 2009 Lisbon.

[10] D.J. Allman, ' A compatible triangular element including vertex rotation for plane elasticity analysis', Computer & Structures, **19**, pp. 1-8, (1984).

[11] L. Malvern, Introduction to the Mechanics of a Continuous Medium, Prentice Hall, (1969), New-York.

[12] Rodrigues O., 'Des lois géometriques qui régissent les déplacements dun système solide dans l'espace ', Journal de Mathématiques Pures et Appliques, 5, (1840), 380-440.

[13] C.C. Rankin, B. Nour-Omid, 'The use of projectors to improve finite element performance', Computer & Structures, **30**, pp. 257-267, (1988).

[14] A. Ibrahimbegović, R. L. Taylor, 'On the role of frame-invariance in structural mechanics models at finite rotations', Computer Methods in Applied Mechanics and Engineering, **191**, pp. 5159-5176, (2002).

[15] M. Y. Kim, S. P. Chang, S. B. Kim, 'Spatial stability of thin-walled space frames' Int. Journal for Numerical Methods in Engineering, **39**, pp. 499-525 (1996)